Chemical Engineering Journal 517 (2025) 164337

Contents lists available at ScienceDirect

Chemical Engineering Journal

journal homepage: www.elsevier.com/locate/cej

Photocatalytic conversion of D5 siloxane in water: An exploratory research and mechanism of the process

Paula Felczak [a], Piotr Miądlicki [a], Gustavo Chacón-Rosales [b], Jacek Przepiórski [a,*]

[a] Department of Catalytic and Sorbent Materials Engineering, Faculty of Chemical Technology and Engineering, West Pomeranian University of Technology in Szczecin, Piastów Ave. 42, 71-065 Szczecin, Poland
[b] Institute of Chemical Technology, Universitat Politècnica de València-Consejo Superior de Investigaciones Científicas (UPV-CSIC), Av. de los Naranjos, 46022 Valencia, Spain

ARTICLE INFO

Keywords:
Siloxanes
Decamethylcyclopentasiloxane (D5)
Photocatalytic conversion
Titanium dioxide
Reaction mechanism

ABSTRACT

Siloxanes, challenging contaminants in biogas, can severely impact the combustion engine performance, necessitating their removal. Typically, siloxanes are removed from biogas through adsorption on activated carbon. However, the potential for eliminating siloxanes from wastewater prior to methane fermentation remains underexplored. Therefore, in this work the possibility of photocatalytic conversion of decamethylcyclopentasiloxane (D5) in aqueous phase using UV radiation and titanium dioxide (TiO_2) as photocatalysts is investigated. The effects of several factors on the process, including the effect of UV light and the presence of the photocatalyst on the reaction pathway are examined. Gained findings indicate that the final product of D5 conversion in the aqueous phase is amorphous silica. Given the non-volatility of this product, results in the context of minimizing undesirable desorption of siloxane from the aqueous phase into the gas phase are discussed. Through a detailed analysis, key intermediate species were identified and a reaction mechanism that elucidates the transformation of D5 under photocatalytic conditions in water is proposed.

1. Introduction

The increasing focus on sustainable solutions in response to environmental issues has led to the exploration of alternative energy sources and waste management strategies. Biogas, produced by anaerobic digestion of organic sources including sewage sludge, animal waste, food waste, and agricultural residues [1] has become an important choice in the production of energy from renewable sources. The use of this method is a way to reduce greenhouse gas emissions through controlled production of methane from organic waste and its use [2,3]. Biogas is typically employed as a fuel for the generation of heat, either through conventional methods involving the use of burners or through the co-generation of heat and electricity using dedicated generators and biogas – fueled engines. Biogas is composed predominantly of methane and carbon dioxide, with smaller amounts of nitrogen and oxygen [4,5]. In addition to its major constituents, biogas contains a range of trace compounds that present technical and environmental challenges. These include primarily hydrogen sulfide [6], ammonia [7], and non-methane volatile organic compounds (NMVOCs) [8]. Knowing the typical composition of biogas is crucial for designing effective strategies for its treatment and utilization. This is because its components determine the conditions for storage and transportation, as well as end use. A representative composition of raw biogas, including both major and trace components, is illustrated in Fig. 1. which can serve as a reference point for assessing the need for gas purification and upgrading.

Due to specific requirements and standards, some of these contaminants need to be eliminated prior to biogas combustion. For example, hydrogen sulfide produces sulfur dioxide upon combustion [9], that is corrosive and poses environmental hazards. It should be noted that recently of special concern are silicon-based compounds, known as siloxanes [4,5,10]. Such structures occurring as cyclic or linear forms are a common component of municipal wastewater [4,5,10]. Examples together with their Henry's law volatility constants and boiling points are shown in Table 1.

The most common siloxanes found in sewage are considered volatile methyl siloxanes (VMS, Table 1). Among them, these of molecular weight below 500 $g \cdot mol^{-1}$ are considered as volatile under normal conditions [13]. Due to their significant volatility, these compounds are

* Corresponding author.
E-mail addresses: paula.felczak@zut.edu.pl (P. Felczak), piotr.miadlicki@zut.edu.pl (P. Miądlicki), gjcharos@itq.upv.es (G. Chacón-Rosales), jacek.przepiorski@zut.edu.pl (J. Przepiórski).

https://doi.org/10.1016/j.cej.2025.164337
Received 25 February 2025; Received in revised form 23 May 2025; Accepted 30 May 2025
Available online 31 May 2025

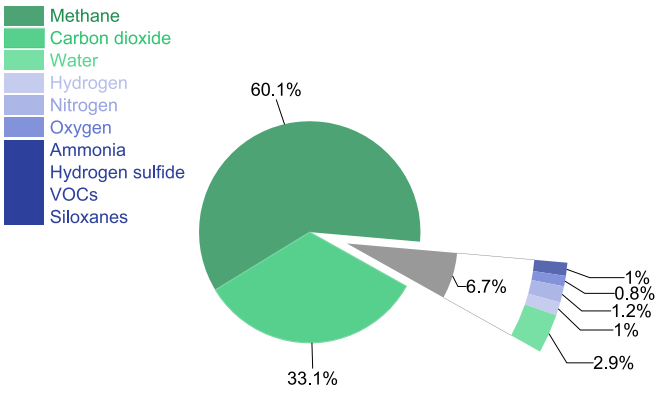

Fig. 1. Approximate biogas composition. []
Adapted from 5–8.

desorbed from the treated wastewater or sewage sludge into the gas phase. This is the reason why siloxanes are often found in raw biogas produced by methane fermentation of sewage sludge. It should be noted that the contents of siloxanes in biogas varies and does not generally correlate with their volatility constants, boiling point or molecular weight. The abundance of siloxanes in biogas depends on the temperature and the concentration in the wastewater. Siloxanes such as D4 and D5 are recognized as the most common in municipal wastewater, mainly due to their extensive use in cosmetics [14].

Combustion of biogas containing siloxanes is accompanied by the formation of silica and silicates, both causing serious technical problems, which occur during the exploitation of biogas-fueled engines [15,16]. Silica crystals formed upon the combustion of biogas cause degradation in engine performance because of abrading engine parts, depressing spark plug functionality, deactivating emission control systems, and contaminating of the engine oil. For these reasons, the removal of siloxanes from biogas is a common and necessary practice, realized through two approaches. The first one, hardly recognized, is a

Table 1
Properties of siloxanes regularly found in municipal wastewaters [11,12].

Siloxane Name	Structure	Boiling point [°C]	Molecular Weight [g·mol^{-1}]	Henry's Law Volatility Constants (H_v)
L2 Hexamethyldisiloxane	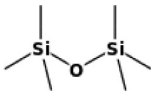	104	162.38	403.4
L3 Octamethyltrisiloxane	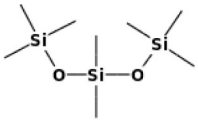	153	236.53	1440.7
L4 Decamethyltetrasiloxane	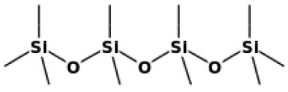	194	310.68	938.1
L5 Dodecamethylpentasiloxane	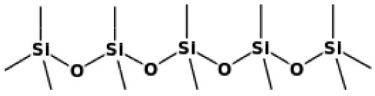	231	384.84	4636.7
D3 Hexamethylcyclotrisiloxane	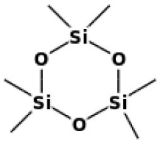	134	222.46	72.0
D4 Octamethylcyclotetrasiloxane	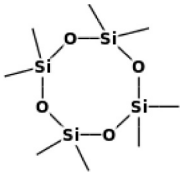	175	296.61	486.0
D5 Decamethylcyclopentasiloxane	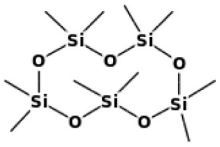	210	370.77	268.9
D6 Dodecamethylcyclohexasiloxane	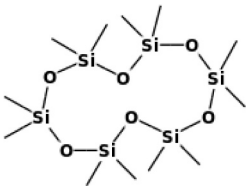	245	444.92	103.4

treatment of wastewater or sewages prior to subjecting them to anaerobic digestion. Another one, well recognized and widely practiced, is the removal of the siloxanes from the produced biogas. The first approach, not practiced, may include processes like biodegradation, gas stripping, and peroxidation [17–19]. In practice, removal of siloxanes has been realized predominantly by adsorption on activated carbon beds where biogas is in contact with the adsorbent [15]. However, despite its popularity, adsorption on activated carbon suffers from the need to regenerate or replace the adsorbent, which generates additional costs [20]. Other commercially available methods also reveal certain drawbacks usually related to unsatisfactory energy consumption, substantial initial and ongoing costs, and operational difficulties [21]. Operational difficulties concern also hardly recognized possibility of photolytic conversion of siloxanes contained in biogas by using UV radiation [22].

The literature review did not provide a satisfactory answer regarding the photocatalytic conversion of siloxanes in an aqueous environment. So far, this process has not been extensively studied, and only a few reports focusing on UV-assisted gas-phase processes in the presence of a photocatalyst were found [23,24]. Sun et al. [23] studied the photocatalytic decomposition of octamethyltrisiloxane (L3) in air on titanium dioxide thin films. It was shown that in the presence of TiO_2 L3 decomposes under the influence of UV radiation, which was confirmed by the decrease in L3 concentration and the accompanying increase in carbon dioxide level. Moreover, the gradual loss of photocatalytic activity of TiO_2 and its complete deactivation due to the formation of hydroxylated silica on its surface were confirmed. Similarly, the deactivation of TiO_2 due to the formation of silica on the surface during the photocatalytic oxidation of octamethylcyclotetrasiloxane (D4) was described by Lamaa et al. [24]. It was also noted that deactivation progressed more rapidly for the higher D4 concentrations used in the study. Both reports propose similar gas-phase reaction mechanisms, according to which the photogenerated hydroxyl radicals attack the methyl groups (−Si-CH_3) of the siloxanes. The effect of this process is the formation of silanol groups (−Si-OH), which undergo further reactions to form silica, that deactivates TiO_2. It should be emphasized, however, that these mechanisms were developed taking into account results of gas-phase experiments. We believe that photocatalytic conversion of siloxanes is also possible in the aqueous phase, and water may act as a medium favoring dispersion of the products formed during the process. Hence, a potential to overcome drawbacks characteristic of the photocatalytic process carried out in the gaseous phase may be expected. For the above reasons, it seems that the approach proposed in this paper, consisting in the conversion of siloxanes into non-volatile products in the aqueous phase, is novel and worth investigating. This work opens a view on the mechanism involved in decomposing troublesome siloxanes by photocatalysis in aqueous environments and opens the way to new strategies in related areas.

2. Experimental

The problem addressed in this work has not been previously studied, and therefore the publication is intended to explain the mechanism of D5 transformations in aqueous phase under photocatalytic conditions. This section provides details of the work and analyses performed, the materials used, and the test conditions and procedures.

2.1. Materials

Photocatalytic conversion studies in aqueous phase were conducted for commercially available D5 siloxane (AmBeed, Inc., 99% purity). D5 is frequently present in municipal wastewater. This siloxane is troublesome in operating activated carbon filters due to such effects as pore clogging or diminishing susceptibility to effective regeneration [15,25]. Moreover, cyclic siloxanes displace linear ones from the pores of activated carbons [15,26] and heavier cyclic siloxanes, such as D5, can displace lighter ones, such as D4 and D3 [27]. Furthermore, cyclic siloxanes, including D5, can undergo polymerization on the surface of activated carbons. For the above reasons, selection of D5 for the preliminary studies seemed to be reasonable and justified.

The titanium dioxide used for the photocatalytic tests was AEROXIDE® P25 (Evonik Operations GmbH 99.5% purity). All the water/siloxane mixtures and water/siloxane/photocatalyst suspensions used in this work were prepared with demineralized water (0.1–0.8 $\mu S \cdot cm^{-1}$). The synthetic air used in the research was of 99.999% purity (Air Liquide). The methanol used for adding to samples subjected to GC/MS analysis (see section 2.3) was HPLC grade (Chempur).

2.2. Experimental setup, sample preparation and conversion procedure

The system used for the tests (Fig. 2) consisted of a 1.5 dm3 glass reactor placed in a thermostatic chamber, equipped with a UV lamp mounted in a quartz immersion tube. A specially constructed, monochromatic UVLED consisting of 32 UVLEDs emitting at 365 ± 5 nm with a radiation intensity of 43 mW cm^{-2} was used for the UV-assisted tests. The lamp was designed to be water-cooled (section S1). The reaction mixture was stirred (ca. 500 rpm) using a magnetic stirrer. Synthetic air was supplied to the reactor in a controlled manner (MFC). The air leaving the reactor was passed through a scrubber with ethanol. The ethanol was analyzed for the possible presence of siloxane and its conversion products that could be desorbed from the mixture in the reactor.

D5/water mixtures were prepared by adding 1 cm^3 of the siloxane to water (1000 cm^3), then sonicating for 60 min. The photocatalyst (quantities shown in Table 2) was then dispersed in this mixture, and the obtained suspension was sonicated for an additional 5 min. The as-prepared mixture was transferred to the reactor and finally placed in a thermostatic chamber in which the temperature of the reaction mixture was maintained at ca. 35°C. During the tests, synthetic air was supplied to the reactor at a flow rate of 0.001 $dm^3 \cdot min^{-1}$. To avoid purging D5 from the mixture, the air flowed over the surface of the liquid.

The intensities of UV light emitted by the lamp were measured in both air and water by using a photo-radiometer (HD2102.1, Senseca Delta OHM) to check how the walls of the quartz tubes and the water influence the intensity of UV radiation supplied to the reaction mixture. The measurements were carried out in three modes: UV sensor was placed next to the lamp with no barrier, in air out of the immersion tube with the lamp inside, and in the water surrounding the tube with the lamp inside. UV intensities were measured at several distances from the radiation source. As shown in Fig. 3, in each mode the UV intensity decreases with distance from the lamp and is not significantly affected by the quartz wall and water. The above observations confirm the efficient UV transport to the D5/water/TiO_2 system in the reactor.

The D5 siloxane conversions in the aqueous phase were carried out using the reaction system described above, under various combinations of conditions, as detailed in Table 2. The selection of conditions was intentional and aimed to provide the results necessary to evaluate the effect of TiO_2 and UV light (on/off) on the conversion of D5 in water.

2.3. Monitoring of D5 conversion progress

To monitor the progress of the D5 conversion, samples (15 cm^3) of the reacting mixtures were taken from the reactor at eight time points: before starting the process and adding photocatalyst to the mixture (0h) and after 0, 3, 6, 9, 24, 30, and 48 h of the processes. 15 cm^3 of methanol was added to each sample to dissolve unreacted siloxane and its conversion products. The mixtures obtained were centrifuged for 30 min (1500 rpm), and the separated liquid was analyzed using GC/MS method. Additionally, after 24 h and 48 h of a process, liquid samples were taken from the ethanol scrubber (see Fig. 2) and analyzed using GC/MS to examine whether siloxane or its conversion products escaped from the reactor. Important details of the measurements and methods are presented in Table 3.

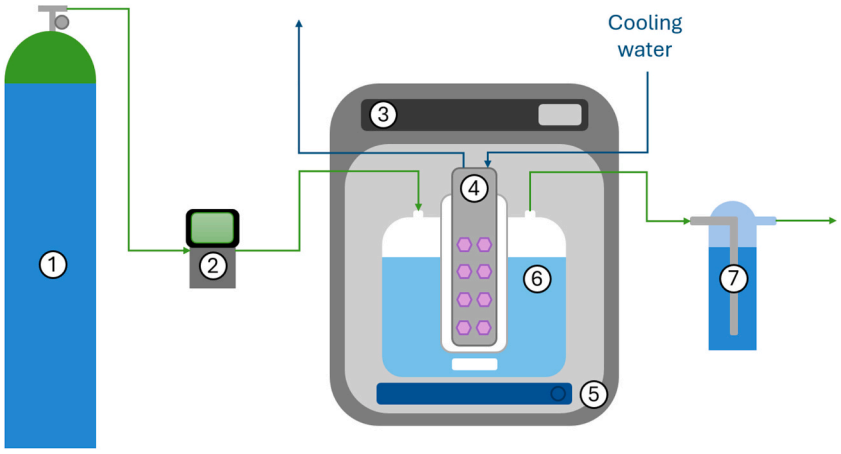

Fig. 2. Experimental setup used for photocatalytic conversion of D5 siloxane in water (1 – synthetic air cylinder, 2 – mass flow controller, 3 – thermostatic chamber, 4 – water-cooled UV-LED lamp, 5 – magnetic stirrer, 6 – reactor, 7 – scrubber).

Table 2
Experimental options used to determine the effects of photocatalyst and UV on conversion of D5 in aqueous phase.

Entry	D5:water, mixture composition, [cm^3:cm^3]	TiO_2 added, [g]	UV irradiation during a test, on/off	Liquid sample symbol	Solid sample symbol
1	1:1000	0.5	on	D5_TiO_2_UV	TiO_2_UV
2	1:1000	0.5	off	D5_TiO_2_wo_UV	TiO_2_wo_UV
3	1:1000	0	on	D5_wo_TiO_2_UV	–
4	1:1000	0	off	D5_wo_TiO_2_wo_UV	–

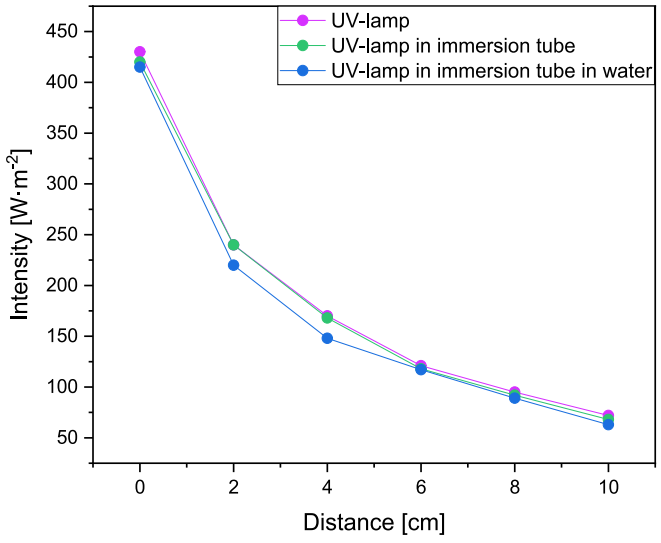

Fig. 3. Change of the UV radiation intensity of the lamp with distance measured in proximity of the lamp without any barrier (purple line), using quartz glass as a barrier (green line), and in water using quartz glass as a barrier (blue line).

2.4. *Characterization of the photocatalyst*

After the D5 siloxane conversion processes, the photocatalysts were separated from the mixtures by centrifugation, dried at 80°C for 24 h, and analyzed by FTIR, XRD, XPS, HRTEM and ^{29}Si NMR. Important details of the measurements and methods are presented in Table 3.

3. Results and discussion

The results of the conducted studies provided a basis for the discussion regarding the effects of photocatalyst and UV radiation on the behavior of D5 siloxane in the aqueous medium. This section focuses on analyzing these results and combining observations to propose a mechanism for the photocatalytic conversion of D5 in water and to draw key conclusions from the conducted research.

3.1. *Changes in D5 contents in reaction mixtures – Effect of reaction conditions*

Results of the GC/MS measurements obtained for samples of the reaction mixtures taken at different times of the conversion processes are shown in Fig. 4.

No significant effect of water alone on the change in the siloxane content of D5 in the system was observed (D5_wo_TiO_2_wo_UV), which is expected due to the low hydrolysis rate of higher cyclic siloxanes, such as D5 [28]. However, the introduction of TiO_2 into the D5/water system resulted in an instant significant reduction in the measured D5 content, both under UV radiation (D5_TiO_2_UV) and without UV (D5_TiO_2_wo_UV). This effect was assumed to result from the adsorption of siloxane on titania. This assumption is supported by the results of FTIR, XPS, and ^{29}Si NMR studies, which are discussed in further sections of the publication (sections: 3.3 FTIR studies, 3.4 XPS studies, and 3.6 ^{29}Si NMR studies). Results of GC/MS analyses indicate a decrease in the content of D5 siloxane along with the duration of the conversion process carried out with the use of UV in both photolytic conditions (without TiO_2), in photocatalytic conditions (with TiO_2) and in the process carried out with only TiO_2. It should be noticed that under the present experimental conditions, the effect of UV is more pronounced in photolytic mode than in the presence of TiO_2. However, the highest decrease in D5 siloxane content relative to the initial value (at 0h) was observed for the photocatalytic process. Considering the above, it can be concluded that during exposure to UV radiation in the presence of TiO_2, both photolytic and photocatalytic processes may occur simultaneously. It should be noted that the results of GC/MS analyses did not show the presence of other compounds than D5 in the mixture after the process. Moreover, by performing GC/MS analyses of ethanol samples taken

Table 3
Details of instrumental methods used during the investigations.

Method	Important details and additional information	Equipment
Fourier Transform Infrared Spectroscopy (FTIR)	Spectra measured in the range of wavenumbers from 400 to 4000 cm^{-1}.	Nicolet iS50 FTIR instrument (Thermo Fisher Scientific, Waltham, MA, USA) equipped with Smart iTR ATR (Thermo Fisher Scientific, Waltham, MA, USA) cell attachment.
X-ray Powder Diffractometry (XRPD)	Diffractograms recorded in the 2θ range 6-100° with a step size of 0.025.	Emperyan X-ray diffractometer (PANanalytical, Almelo, The Netherlands) with Cu K_α radiation source (λ = 0.154 nm, 35 kV, 30 mA). The diffraction data was analyzed using the ICDD PDF 5 + 2024 database and HighScore Plus software (Newtown Square, PA, USA). Rietveld refinement was applied to determine crystalline phase compositions.
X-ray Photoelectron Spectroscopy (XPS)	Measurements were carried out under a high vacuum of ca. 10^{-9} mbar and at 25 °C using non-monochromatic Al K_α X-ray radiation with an energy of 1486.60 eV. During the processing of the XPS spectra, binding energy (BE) values were referenced to the adventitious C1s peak (285 eV).	PHOIBOS 150 MCD 9 analyzer (SPECS, Berlin, Germany). CasaXPS software (Casa Software Ltd.) and the NIST XPS Database library were used for analysis of XPS data.
Solid-State Nuclear Magnetic Resonance (SS-NMR)	Solid-state NMR spectra were recorded at room temperature under magic angle spinning (MAS). 29Si MAS NMR spectra were carried out in a 7.0 mm probe with a 3.5 μs pulse length corresponding to a 60° flip angle, spinal proton decoupling with 60 s as a recycle delay, spinning the sample at 5 kHz. 1H/29Si CP MAS NMR was carried out on a 7.0 mm probe spinning the sample at 5 kHz, using a 1H π/2 pulse length of 4 μs with spinal proton decoupling, 3.5 ms as contact time and 3 s as recycle delay. 1H/13C CP MAS NMR were carried out on a 4.0 mm probe spinning the sample at 10 kHz, using a 1H π/2 pulse length of 2.5 μs with spinal proton decoupling, 2 ms as contact time, and 3 s as recycle delay. The 13C and 29Si NMR spectra were referenced to adamantane and TMS, respectively.	Avance III HD 400 MHz WB spectrometer (Bruker, Billerica, MA, USA).
High-Resolution Transmission Electron Microscopy (HRTEM)	Observations were carried out at an accelerating voltage of 300 kV. High-Angle Annular Dark-Field Scanning Transmission Electron Microscopy (HAADF-STEM) imaging and elemental mapping were performed, employing Scanning Transmission Electron Microscopy with Energy Dispersive Spectroscopy (STEM-EDS). For analyses samples were directly deposited onto copper grids.	Spectra 300 microscope (Thermo Fisher Scientific, Waltham, MA, USA).
Gas Chromatography/ Mass Spectrometry (GC/MS)	The chromatographic conditions were: injection volume 0.5 μL; injector temperature 250 °C; He 6.0 carrier gas in a flow rate 0.94 $cm^3 \cdot min^{-1}$; column temperature program: isothermal at 40 °C for 2 min, temperature rise 10 °C·min^{-1} up to 300 °C, isothermal at 300 °C for 2 min; interface temperature between GC and MS: 250 °C; ion source temperature 200 °C.	Nexis GC-2030 gas chromatograph (Shimadzu, Kyoto, Japan) equipped with an SH-I-5MS (30x0.25x0.25) chromatographic column and coupled to the GCMS-QP2020 NX mass spectrometer (Shimadzu, Kyoto, Japan).

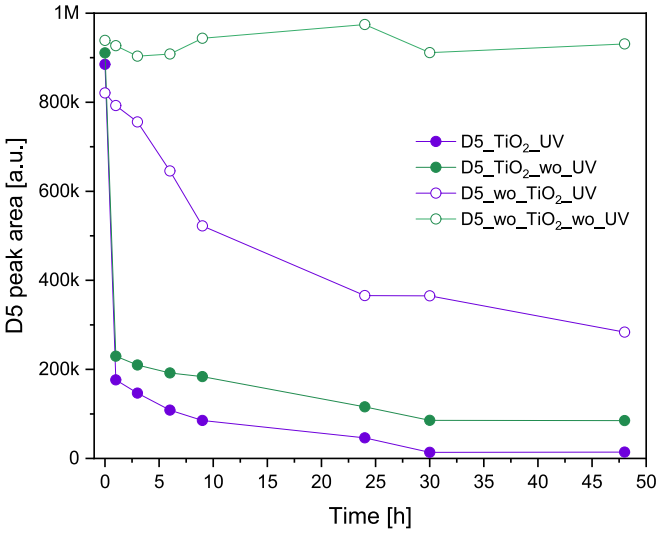

Fig. 4. Change in the GC/MS peak areas from D5 siloxane with time of the conversion processes under different experimental options.

from the scrubber (see Fig. 2), no transport of silicon compounds from the reactor to the scrubber was confirmed. Based on the above-mentioned observations, assumption that the D5 undergoes conversion to high-molecular-weight, non-volatile, and/or water-insoluble compounds was feasible. However, due to the lack of convincing results, it became necessary to conduct further studies to clarify the chain of possible reactions in detail.

3.2. XRD studies

XRD patterns (Fig. 5) were measured to verify the formation of crystalline products potentially formed from the siloxane used in the research, as the literature indicates the formation of the crystalline silica on the surface of the photocatalyst during the photocatalytic conversion of siloxanes in air [24,29].

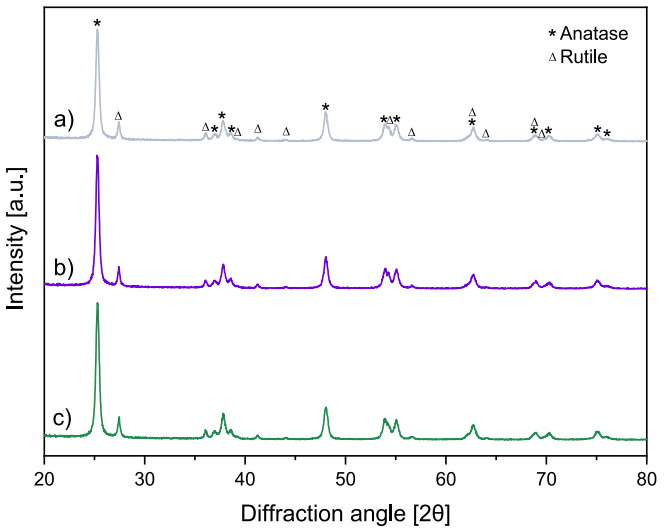

Fig. 5. XRD patterns of TiO_2 used in experiments: a) pristine, b) after 48 h long D5 siloxane conversion process under UV, and c) after 48 h long D5 siloxane conversion process without UV.

Regardless of the experimental conditions, the only phases confirmed in all the examined titania were anatase (ca. 86%) and rutile (ca. 14%). Nevertheless, given the inherent limitations of the XRD method, the possibility of the formation of a new crystalline phase during a process cannot be discounted. For that reason, additional research was undertaken on the formation of a crystalline phase during a process and solids gained during experiments. To do so, further analyses including FTIR, XPS, ^{29}Si NMR and HRTEM have been carried out.

3.3. FTIR studies

FTIR spectra measured for photocatalyst after 48 h of photocatalytic conversion of D5 under UV radiation (TiO_2_UV) and without UV (TiO_2_wo_UV) are presented in Fig. 6.

Distinct differences can be observed at wave numbers ranging from 750 cm^{-1} to 1450 cm^{-1}. In the case of the as-measured FTIR spectrum of the TiO_2 after the process in the presence of UV (Fig. 6a), apparent absorption bands corresponding to stretching vibrations of Si-O-Si groups (1010–1170 cm^{-1} [30–33]) and low intensity bands corresponding to stretching vibrations of Si-CH_3 groups (1266 cm^{-1} [31,33]), can be observed. This observation may indicate the presence of both organosilicon compounds and inorganic silicon compounds in the measured material. On the other hand, the FTIR spectrum of TiO_2_wo_UV, reveals the presence of absorption bands resulting from stretching vibrations of CH_2 groups (1416 cm^{-1} [31,32,34]) and symmetric stretching vibrations of COO groups (1341 cm^{-1} [35]). Considering the literature reports on the oxidation of D5 siloxane, this may indicate the formation and presence of organic compounds such as formaldehyde or formic acid [36,37]. No evident, however signals in the 900–1200 cm^{-1} region, corresponding to the presence of Si-containing groups (such as Si-O-Si, Si-CH_3) were detected in case of the FTIR spectrum of TiO_2_wo_UV. Because the partial sorption of D5 takes place on the photocatalyst (see Fig. 4), confirmation of the presence of these groups was expected. Therefore, to gain more from attained spectral data, the FTIR spectrum of P25 was subtracted from the spectra of photocatalysts after use. Thus, FTIR signals corresponding to the species adsorbed on the titania could be observed (Fig. 6b). The subtracted spectra of both materials revealed bands corresponding to stretching vibrations of three kinds of groups, i.e. Si-O-Si (1020–1135 cm^{-1} [30–33]), Si-OH (940 cm^{-1} [42]), and Si-CH_3 (1268 cm^{-1} and 790 cm^{-1}[31–33]). Intensive bands corresponding to Si-CH_3 stretching vibrations in the spectrum of the material after the process carried out without UV and intense bands corresponding to the stretching vibrations of Si-O-Si and Si-OH groups in the material after the process using UV, indicate significant differences in the chemistry of these processes. The observation of structures containing Si-CH_3 groups may indicate the presence of unreacted siloxane D5 and/or other organosilicon compounds. On the other hand, the rounded band from the Si-O-Si and Si-OH groups is characteristic of silica and may indicate its presence on the photocatalyst surface [38]. However, the uncertainty of the conclusion required further analysis. The band assignments for the FTIR spectra shown in the graphs (Fig. 6) are summarized in Table S1 (Section S2).

3.4. XPS studies

XPS measurements (results shown in Fig. 7) were conducted to determine the surface elemental composition of photocatalysts, both prior to and after use in the processes, and to examine the presence of possible silicon compounds, including adsorbed D5 and products formed from the siloxane during treatment at different experimental conditions.

The XPS analyses of the O 1s and Si 2p spectral regions reveal significant differences in the surface chemistry of the tested samples after their use in the D5 conversion process (Fig. 7). These differences are associated with the treatment of UV radiation during the conversion. As expected, all the samples studied showed the presence of a dominant Ti-O band at 530.1 eV in the XPS O 1s spectral region, characteristic of TiO_2 [39]. The XPS spectrum of the titania sample, after D5 conversion

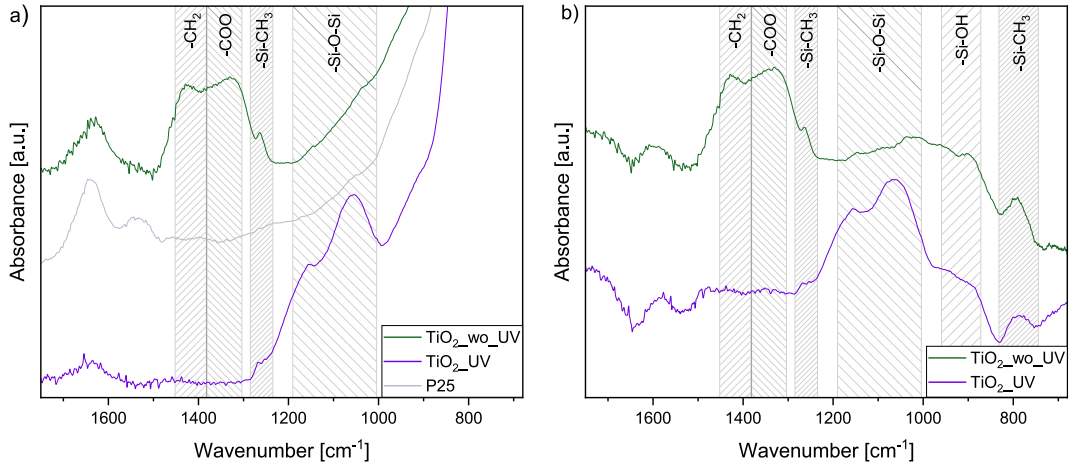

Fig. 6. FTIR spectra of P25 TiO_2 after 48 h of D5 siloxane conversion process under UV (TiO_2_UV) and without UV (TiO_2_wo UV): a) as measured and b) after subtracting the FTIR spectrum of the commercial P25 (Fig. 6a, grey line).

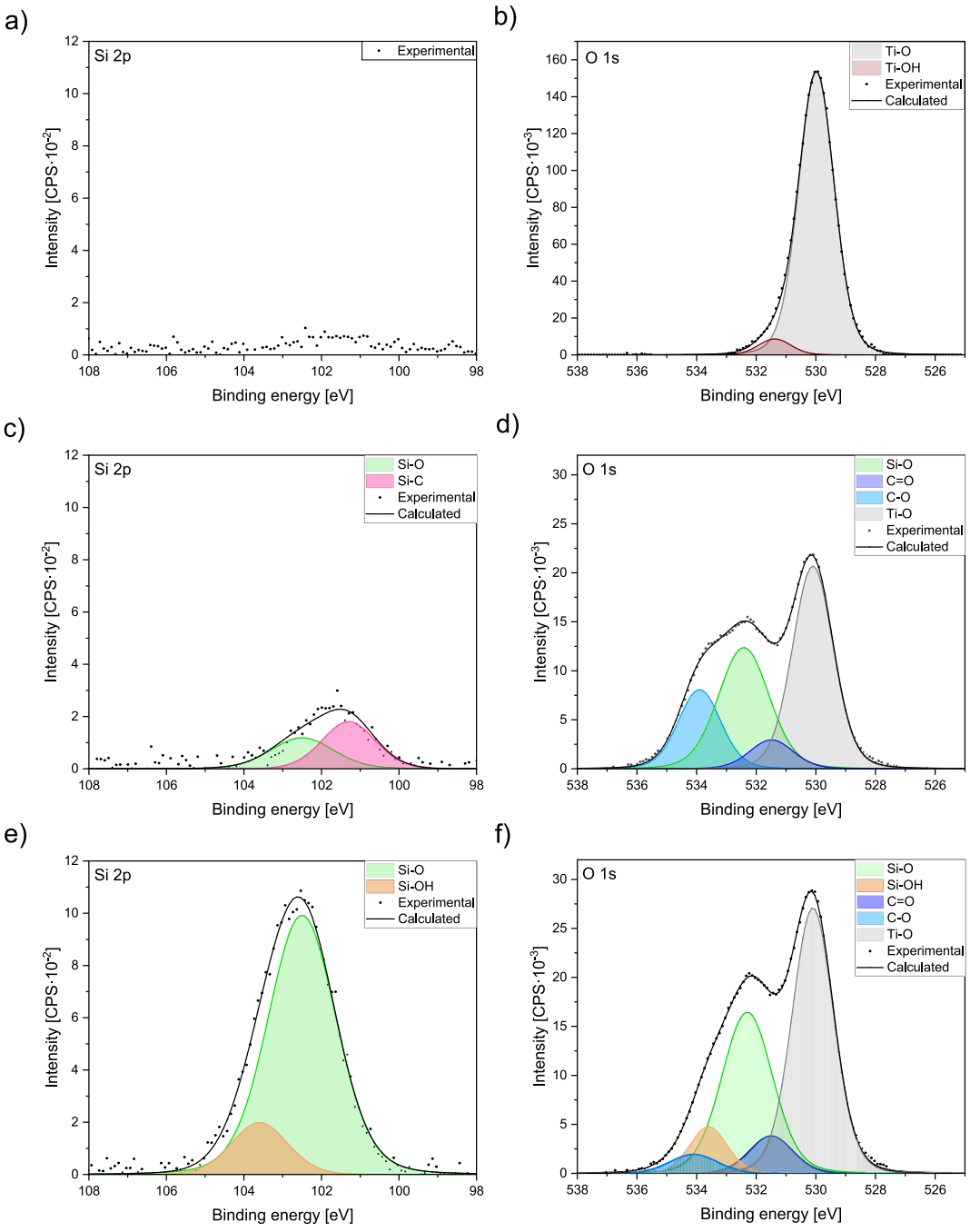

Fig. 7. XPS spectra (Si 2p and O 1 s regions) P25 photocatalyst: pristine a), b), after 48 h of the process carried out without UV (TiO_2_wo_UV) c), d) and after 48 h of the process carried out under UV irradiation (TiO_2_UV) e), f).

carried out without UV irradiation (TiO_2_wo_UV), exhibited notable differences from pristine P25. Analysis of the O 1s region of the XPS spectrum showed the presence of a signal centered at 532.4 eV, characteristic of Si-O bonds [24], as well as two signals at 533.9 eV and 531.5 eV, which corresponds to two new chemical bonds C-O [40] and C=O [41], respectively. It is noteworthy that the presence of a signal from Si-O bonds (102.5 eV [23,24]) together with the concurrently observed XPS signal in the Si 2p region (101.3 eV, Fig. 7c), denotes the presence of Si-C bonds in the tested material [42]. This observation can be attributed to organosilicon compounds at the surface, including unreacted D5 siloxane and/or its conversion products. On the other hand, the XPS signals attributed to C-O bonds (533.9 eV) suggest the presence of organic compounds containing oxygen. Considering the composition of the whole reacting system, by-products of the D5 conversion seem to be formed. As reported elsewhere, forming •OH radicals under photolytic conditions can favor the D5 decomposition to formaldehyde and formic acid [36,37], which can further react with TiO_2 to form surface functional groups [34,35,43].

For comparison, the results of XPS analysis developed the photocatalyst sample after the D5 conversion carried out in the presence of UV radiation (TiO_2_UV) indicate a different transformation path of the siloxane. Well-defined XPS O1s signals at 532.4 eV and 533.6 eV can be attributed to Si-O and Si-OH bonds, respectively (Fig. 7f). Such a pattern was reported as characteristic of silica [44,45]. In addition, the presence of distinct signals in the Si 2p region at 102.5 eV and 103.6 eV, can be attributed to the respective Si-O and Si-OH groups, species naturally

present in the silica structure [23,24,46,47]. The lack of notable evidence of Si-C bonds in Fig. 7e may be another confirmation of silica formation. Comparative analysis of the XPS spectra of TiO_2_wo_UV and TiO_2_UV allows us to conclude that UV irradiation promotes the formation of silica in the D5/TiO_2/water system. This is evidenced by the decreased intensity of the XPS signal observed in the O 1s region for the TiO_2_UV sample, indicating a lower content of C-O bonds. Moreover, a significant increase in the XPS signal intensity in the Si 2p region suggests a higher content of Si-O bonds. It should be noted that none of the XPS spectra of the examined solids revealed signals characteristic of Ti-Si bonds (98.6 eV [48]). The absence of Ti-Si bonds, as shown by XPS analyses, provides evidence that silica and/or oligomeric siloxanes are formed on the TiO_2 surface as separate components and are not incorporated into the catalyst lattice. This effect has been discussed in section 4 of this work (4. Mechanism of D5 siloxane conversion in water).

3.5. TEM observations

HRTEM images of photocatalysts, both pristine and after the D5 conversion process, are presented in Fig. 8. In the photocatalyst samples after the process was carried out without the use of UV radiation, no components other than P25 were detected (Fig. 8a and Fig. 8c). However, in the photocatalyst sample separated from the reaction mixture exposed to UV radiation, the presence of irregular amorphous forms on its surface (marked with an arrow in Fig. 8b) was confirmed. The results of HAADF-STEM imaging and STEM-EDS mapping showed that the photocatalyst contained dopants in the form of silicon compounds (Fig. 9c and Fig. 9d). In turn, the result of comparing the TiO_2 mapping images after the process carried out under UV light (Fig. 9d) and without this radiation (Fig. 9b) indicates that the use of UV results in the accumulation of silicon compounds in larger amount.

3.6. ^{29}Si NMR studies

Due to the lack of convincing conclusions from XPS, XRD, FTIR, and other analyses, ^{29}Si NMR measurements were carried out. Their aim was to confirm whether the differences observed in photocatalyst samples both exposed to UV radiation and without it were significant and whether these differences were helpful in explaining the D5 conversion mechanism. Furthermore, it could be expected that the results of NMR analyses would provide a better understanding of the course of photocatalytic conversion over time. The observations from the ^{29}Si NMR spectra obtained for TiO_2 samples after different times (24, 48 and 168 h) of photocatalytic D5 conversion (Fig. 10) indicate significant progress of the reaction over time. In turn, the spectrum of the photocatalyst after the process carried out without the use of UV (TiO_2_wo_UV) provides clear confirmation of the absence or presence of only traces of silica and thus the key influence of this radiation on the D5 conversion mechanism.

In the ^{29}Si NMR spectrum of the photocatalyst after 24-hours-long process, multiple prominent signals are observed between −10 and −120 ppm. The low-field signals up to −20 ppm correspond to the characteristic D5 siloxane ones, representative of the Si=$(CH_3)_2$ groups in their initial structure. The signals in the range of −50 ppm and −70 ppm, correspond to intermediate T^n-type (T^1, T^2Ti, T^2Si and, T^3), silanol (Si-OH) species [49] interacting with TiO_2 surface (Fig. 11). It is worth noting that TiO_2 especially under UV radiation can generate both •OH and $\bullet O_2^-$ radicals, which facilitate the fragmentation of Si–CH_3 bonds. The interaction of these reactive species with surface Ti–OH sites on TiO_2 leads to the formation of Ti-O-Si species. Studies have shown that the presence of hydroxyl radicals, along with defects such as oxygen vacancies and Ti^{3+} centers generated during the photocatalytic process, enhance charge separation and increase the reactivity of TiO_2, thereby promoting the degradation of organic compounds [50,51].

Signals associated with T-type species suggest that D5 siloxane adsorbed on the photocatalyst surface undergoes reactions leading to the formation of silanol species bound to TiO_2 through Ti–O–Si bonds. These signals may also indicate partial cleavage of Si–O–Si bonds in D5, resulting in the formation of linear siloxanes. However, no other organosilicon compounds besides D5 siloxane were identified during the performed processes, making this hypothesis difficult to confirm. Notably, the appearance of signals in the range of –50 ppm to –70 ppm suggests interactions between intermediate products and TiO_2, potentially mediated by hydroxyl radicals generated during UV irradiation, like those observed for D4 siloxane [24,52]. Prominent signals centered at –90.2, –100.8, and –109.3 ppm correspond to the formation of Q^2 [Si$(OSi)_2(OH)_2$], Q^3 [Si$(OSi)_3(OH)$], and Q^4 [Si$(OSi)_4$] intermediates (Fig. 12), respectively. These structures arise from the partial condensation of D5[53], facilitated by interactions between the conversion products and the TiO_2 surface.

The ^{29}Si NMR analysis of the photocatalyst after 48 h of photocatalytic conversion of D5 reveals a significant decrease in signals within the –40 ppm to –70 ppm range. The disappearance of these signals indicates the transient nature of the silanol species and the surface bonds between the photocatalyst and D5 conversion products (Ti–O–Si) [37,54]. After 168 h of the process, the ^{29}Si NMR spectrum of the photocatalyst exhibits evident signals only between –10 and –20 ppm and at –100 ppm, suggesting the progression of intermediate product transformations toward more stable states.

The results observed for D5 siloxane, could be associated with this specific restructuring of the catalyst surface, the modification of the electronic properties [55], interactions between active species and reactants or products [56–58] and adjustments in the electronic and structural properties of active sites [59,60]. The findings described above underscore the importance of long-term monitoring to understand the dynamics of the photocatalytic process and its relationship to catalytic activity and stability under operational conditions.

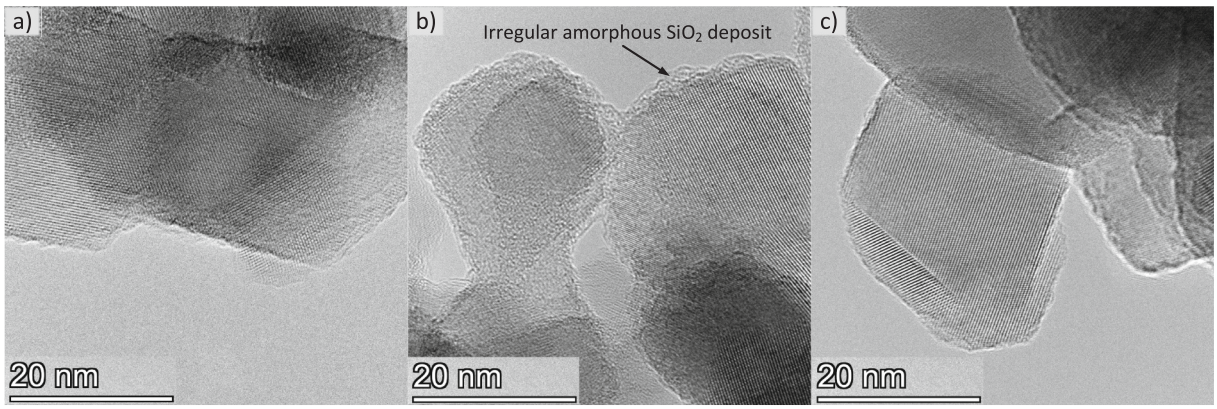

Fig. 8. HRTEM images of the photocatalyst: pristine P25 a), after 48 h of the D5 siloxane conversion carried out under UV radiation b) and, without UV radiation c).

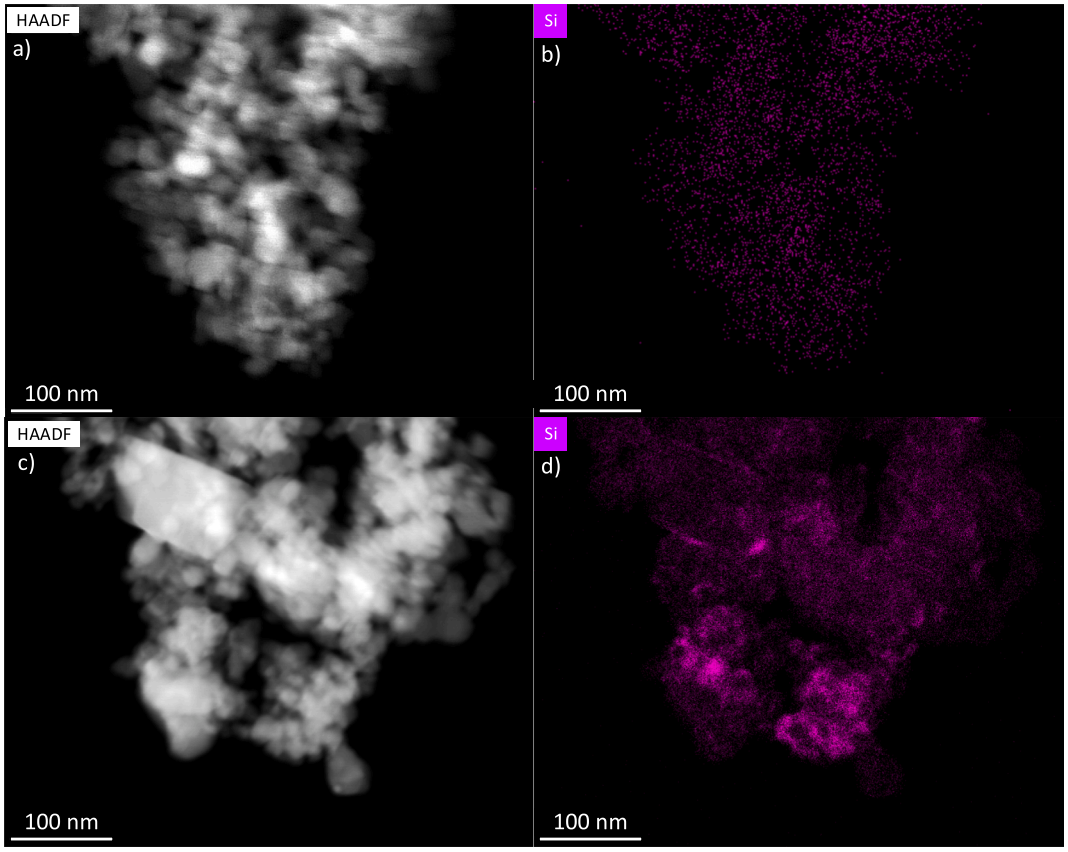

Fig. 9. HAADF-STEM images of TiO_2 after 48 h of the photocatalytic conversion of D5 siloxane carried out without UV radiation a) and under UV c), with corresponding silicon mappings b), d).

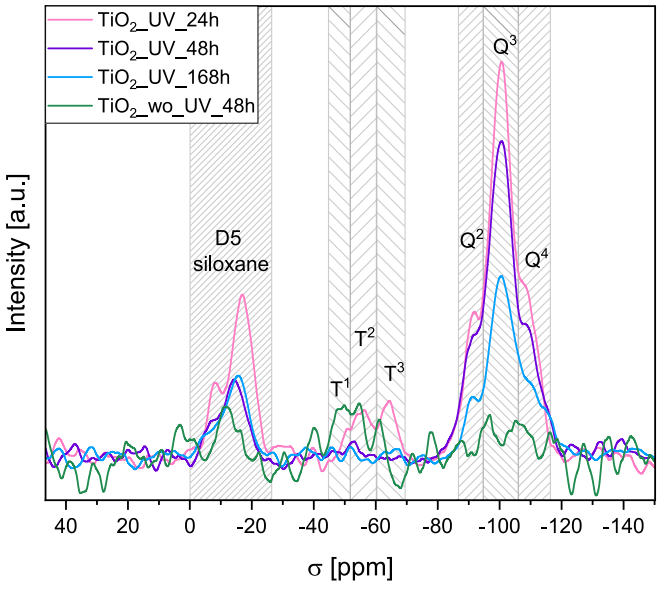

Fig. 10. ^{29}Si NMR spectra of the photocatalysts after D5 siloxane conversion process carried out with UV radiation. The spectrum of TiO_2_wo_UV is presented for comparison.

It is important to note that due to the low amount of silicon deposited because of D5 siloxane degradation, the solid-state 29Si NMR signals were remarkably weak. To improve the signal-to-noise ratio, the cross-polarization magic-angle rotation (CP-MAS) technique was employed, and spectra were accumulated over 24 h. Despite this time, the low signal intensity prevented reliable quantitative or semi-quantitative analysis of T- and Q-type species. For these reasons, the results presented are limited to a qualitative assignment of the silicon species present, based on their characteristic chemical shifts.

4. Mechanism of D5 siloxane conversion in water

Given the evidence presented in this paper, it became possible to propose the mechanism. It also became clear that D5 in water phase may undergo chemical reactions depending on the conditions applied. In contrast, in the absence of both TiO_2 and UV irradiation, the D5 was stable (Fig. 4), which is to be expected due to its low hydrolysis potential [28].

4.1. Mechanism of D5 conversion in water: Effect of UV

In the reaction of D5 siloxane with •OH radicals, siloxanyl radicals are formed, which then undergo transformations into silanols and volatile organic compounds, such as formaldehyde and formic acid [37,61]. The resulting products can undergo further degradation to low molecular weight compounds, such as SiO_2 and CO_2 [37,61]. It should be noted that previous studies have mainly focused on gas-phase reactions of siloxanes using UVB/UVC radiation, while our current study uses UVA radiation in the aqueous phase. This difference may cause different conversion pathways. Therefore, future studies should aim to investigate the conversion pathways of siloxane D5 under different types of UV, which will allow for a better understanding of the transformation behavior of this compound under photolytic conditions.

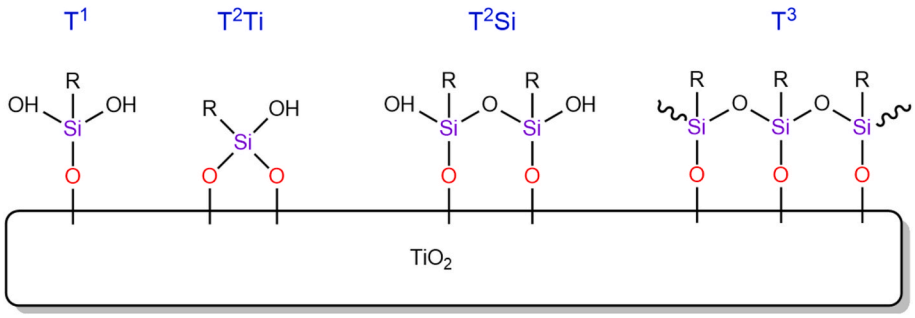

Fig. 11. Proposed structures on the TiO_2 surface, formed during photocatalytic transformations of D5 siloxane: T^n-type intermediates (T^1, T^2Ti, T^2Si, and T^3) silanol (Si–OH) species.

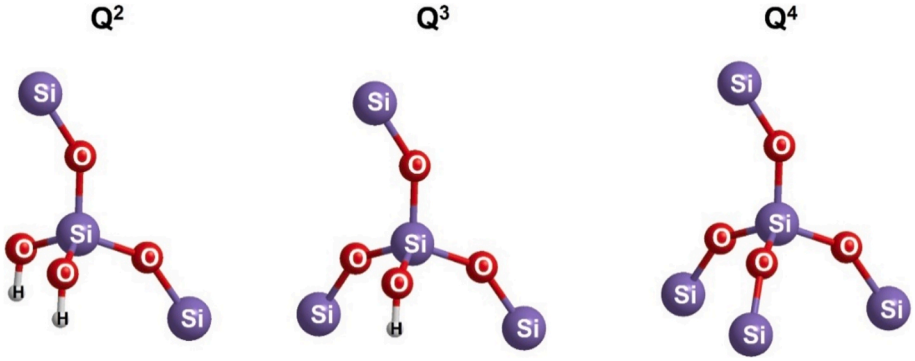

Fig. 12. Proposed intermediate Q-type structures (Si-O-Si) as products of partial D5 condensation carried out under photocatalytic conditions.

4.2. *Mechanism of D5 conversion in water: Effect of UV and TiO_2*

The proposed mechanism of D5 siloxane conversion in water under photocatalytic conditions is illustrated by the scheme presented in Fig. 13. Based on the obtained results, it is reasonable to conclude that D5 is converted to a greater extent under photocatalytic conditions than during conversion processes conducted using only UV or photocatalyst. This is due to the synergistic effect of photolysis and photocatalysis, which increases the intensity of radical generation in the reaction environment. It is reasonable to assume that the introduction of the photocatalyst to the D5/water system is accompanied by adsorption of D5 siloxane on the TiO_2 surface. During the photocatalytic conversion of

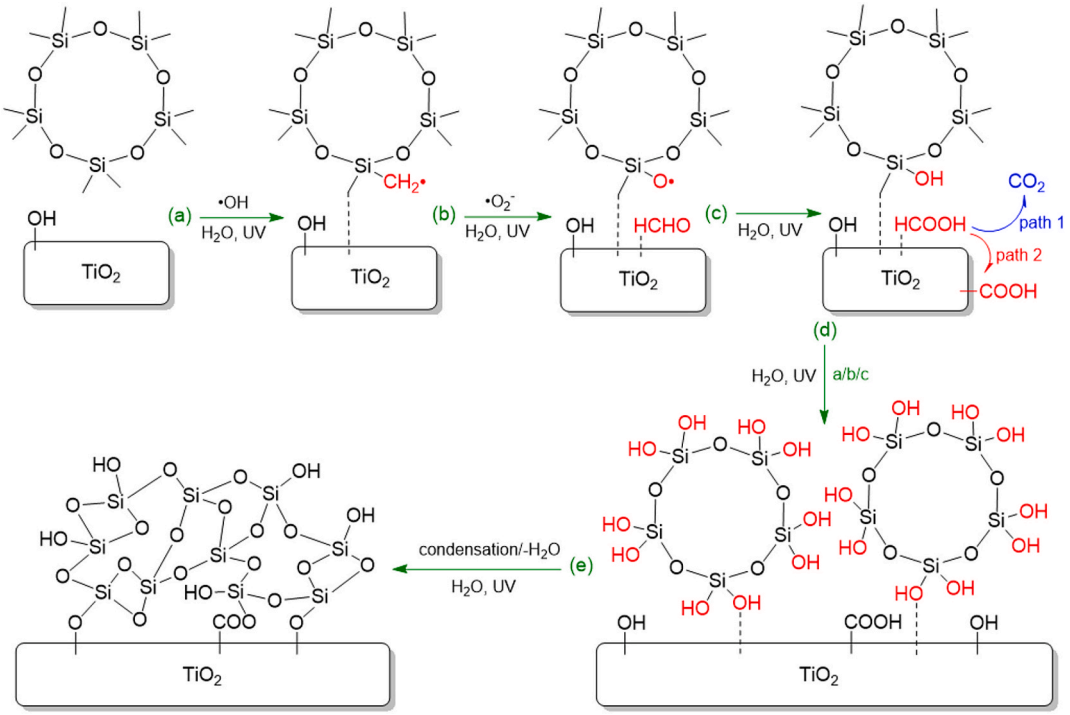

Fig. 13. Proposed mechanism for photocatalytic conversion of D5 siloxane in water.

D5 siloxane, hydroxyl radicals (•OH) formed on the TiO_2 surface attack the methyl group in the structure of the adsorbed D5 siloxane, resulting in the formation of D5-CH_2• radicals (a). Then, D5-CH_2• radicals react with superoxide anion (•O_2–), generated as a result of the reduction process of oxygen molecules on the photocatalyst surface (b). The effect of this reaction is the formation of D5-O• radical and formaldehyde, which is adsorbed on the photocatalyst surface. The D5-O• radicals that are formed react with water, which is the reaction medium, resulting in the formation of hydroxyl groups, while the adsorbed formaldehyde is oxidized to formic acid (c). As a result, D5 siloxane is converted to D5-OH silanol. Formic acid adsorbed on the photocatalyst surface can undergo further photocatalytic oxidation to CO_2 (path 1) or permanently bind to TiO_2, thus forming surface carboxyl groups (path 2). The remaining methyl groups in the formed D5-OH silanol undergo reactions (a-c), which results in the formation of further hydroxyl groups in the molecules of the structure (d). The resulting hydroxyl groups in the silanol can also undergo condensation: with Ti-OH groups on the TiO_2 surface, with carboxyl groups, and also with –OH groups of the same molecule or other silanols, which leads to the formation of amorphous silica on the photocatalyst surface (e).

4.3. Mechanism of D5 conversion in water: Effect of TiO_2

In the process conducted with the photocatalyst without UV radiation, D5 siloxane adsorption was also observed. After the workup and the corresponding characterization of the TiO_2_wo_UV photocatalyst (FTIR, XPS, ^{29}Si NMR), the results led us to conclude that some portion of the D5 siloxane had already desorbed. It should be emphasized that the reaction routes on the photocatalyst surface without the use of UV and in the presence of the radiation, are different. In the case of the process carried out using TiO_2 without UV radiation, siloxane D5 after being adsorbed on the photocatalyst surface reacts according to the path (a) → (b) → (c) (Fig. 13), whereby due to the absence of UV the formation of •OH and •O_2– radicals is limited, which does not favor the conversion of –CH_3 groups to –OH in the siloxane. As a consequence, no further reactions leading to the formation of silanols with a higher content of –OH groups take place, nor does the condensation of silanols occur. For this reason, in the absence of UV radiation, silica formation does not take place. Moreover, the oxidation of organic compounds (formaldehyde and formic acid) is inefficient, which leads to a higher content of C–O and C=O groups in the photocatalyst (TiO_2_wo_UV), which is confirmed by the results of XPS analyses.

5. Conclusions

Considering the obtained and analyzed research results and knowledge from available literature, several key insights into the photocatalytic transformation of D5 siloxane can be concluded. Under our reaction conditions, D5 in the aqueous phase can be effectively converted into amorphous silica, a stable, non-volatile residue that remains in the reaction medium. This mechanism pathway proposed offers a potential strategy to retain siloxane in the aqueous phase, thus minimizing its release into the gas phase and avoiding more complex removal techniques. Significantly, intermediates such as formaldehyde and formic acid are oxidized to CO_2, reducing the risk of accumulating harmful by-products in the effluents. These results, although obtained under controlled conditions with pure water and a single target contaminant, provide a strong foundation for future applications. They offer a clear and well-understood model that can now be expanded to more complex wastewater scenarios, where D5 siloxane coexists with other organic compounds. This controlled baseline is essential to guide the rational design of photocatalytic systems for more complex environments. It's also worth noting that no significant conversion to silica occurs under only UV light (absence of TiO_2) and that in dark conditions, D5 is exclusively adsorbed onto the TiO_2 surface. These observations are critical when designing practical treatment systems and planning future research, particularly regarding the behavior of other siloxanes under similar conditions. This area remains to be explored experimentally.

Future research work should focus on extending presented findings to more complex aqueous matrices, exploring competitive adsorption and degradation in the presence of multiple siloxanes and organic pollutants. Applying this photocatalytic strategy in continuous-flow systems or under solar irradiation could also bridge the gap between laboratory studies and scalable environmental applications.

CRediT authorship contribution statement

Paula Felczak: Writing – review & editing, Writing – original draft, Visualization, Validation, Methodology, Investigation, Formal analysis, Data curation, Conceptualization. **Piotr Miądlicki:** Writing – review & editing, Writing – original draft, Visualization, Validation, Methodology, Investigation, Formal analysis, Data curation, Conceptualization. **Gustavo Chacón-Rosales:** Writing – review & editing, Writing – original draft, Visualization, Validation, Methodology, Investigation, Formal analysis, Data curation, Conceptualization. **Jacek Przepiórski:** Writing – review & editing, Writing – original draft, Validation, Supervision, Resources, Project administration, Methodology, Investigation, Funding acquisition, Conceptualization.

Declaration of competing interest

The authors declare the following financial interests/personal relationships which may be considered as potential competing interests: Jacek Przepiórski reports financial support was provided by National Science Centre Poland. If there are other authors, they declare that they have no known competing financial interests or personal relationships that could have appeared to influence the work reported in this paper.

Acknowledgements

This research was funded by National Science Centre, Poland, grant no. 2022/47/O/ST8/03074.

G.C-R thanks to the FGCSIC ComFuturo /Horizon 2020 program (MSCA grant agreement No. 10103426) for fellowship support during this investigation and extends special thanks to José Alejandro Vidal-Moya for his valuable assistance with the CP-MAS NMR measurements and insightful comments.

P.F. thanks Aleksander Albrecht for valuable comments in the context of XPS results.

Transmission Electron Microscopy (TEM) analyses have been conducted at the Center for Advanced Materials and Manufacturing Process Engineering (CAMMPE; WPUT in Szczecin, Poland).

Appendix A. Supplementary data

Supplementary data to this article can be found online at https://doi.org/10.1016/j.cej.2025.164337.

Data availability

Data will be made available on request.

References

[1] T. Al Seadi, D. Rutz, R. Janssen, B. Drosg, Biomass resources for biogas production, in: The Biogas Handbook: Science, Production and Applications, Elsevier Inc., 2013: pp. 19–51. doi: 10.1533/9780857097415.1.19.

[2] R. O'Shea, R. Lin, D.M. Wall, J.D. Browne, J.D. Murphy, Using biogas to reduce natural gas consumption and greenhouse gas emissions at a large distillery, Appl. Energy 279 (2020), https://doi.org/10.1016/j.apenergy.2020.115812.

[3] A. Elizabeth Funmi, M. Abiodun Suleiman, O. Inioluwa Deborah, A. Tofunmi Dorcas, Biogas production as energy source and strategy for managing waste and climate change, SN Appl Sci 3 (2021). doi: 10.1007/s42452-020-03973-8.

[4] A. Calbry-Muzyka, H. Madi, F. Rüsch-Pfund, M. Gandiglio, S. Biollaz, Biogas composition from agricultural sources and organic fraction of municipal solid waste, Renew Energy 181 (2022) 1000–1007, https://doi.org/10.1016/j.renene.2021.09.100.
[5] J.K. Heffernan, C.-Y. Lai, R.A. Gonzalez-Garcia, L. Keld Nielsen, J. Guo, E. Marcellin, Biogas upgrading using Clostridium autoethanogenum for value-added products, Chemical Engineering Journal 452 (2023) 138950, https://doi.org/10.1016/j.cej.2022.138950.
[6] F. Egger, T. Hülsen, D.J. Batstone, Continuous H2S removal from biogas using purple phototrophic bacteria, Chem. Eng. J. 454 (2023) 140449, https://doi.org/10.1016/j.cej.2022.140449.
[7] X.Y. Chen, H. Vinh-Thang, A.A. Ramirez, D. Rodrigue, S. Kaliaguine, Membrane gas separation technologies for biogas upgrading, RSC Adv. 5 (2015) 24399–24448, https://doi.org/10.1039/C5RA00666J.
[8] J.I. Salazar Gómez, H. Lohmann, J. Krassowski, Determination of volatile organic compounds from biowaste and co-fermentation biogas plants by single-sorbent adsorption, Chemosphere 153 (2016) 48–57, https://doi.org/10.1016/j.chemosphere.2016.02.128.
[9] R.A.S. Lestari, W.B. Sediawan, S. Syamsiah, J.A.T. Sarto, Hydrogen sulfide removal from biogas using a salak fruit seeds packed bed reactor with sulfur oxidizing bacteria as biofilm, J Environ Chem Eng 4 (2016) 2370–2377, https://doi.org/10.1016/j.jece.2016.04.014.
[10] D. Foppiano, M. Tarik, J. Schneebeli, A. Calbry-Muzyka, S. Biollaz, C. Ludwig, Siloxane compounds in biogas from manure and mixed organic waste: Method development and speciation analysis with GC-ICP-MS, Talanta 208 (2020) 120398, https://doi.org/10.1016/j.talanta.2019.120398.
[11] S. Kim, J. Chen, T. Cheng, A. Gindulyte, J. He, S. He, Q. Li, B.A. Shoemaker, P.A. Thiessen, B. Yu, L. Zaslavsky, J. Zhang, E.E. Bolton, PubChem 2023 update, Nucleic Acids Res 51 (2023) D1373–D1380. doi: 10.1093/nar/gkac956.
[12] R. Sander, Compilation of Henry's law constants (version 5.0.0) for water as solvent, Atmos, Chem. Phys. 23 (2023) 10901–12440, https://doi.org/10.5194/acp-23-10901-2023.
[13] C. Pascual, S. Cantera, R. Lebrero, Volatile Siloxanes Emissions: Impact and Sustainable Abatement, Perspectives (2021) 1245–1248, https://doi.org/10.1016/j.tibtech.2021.05.003.
[14] E.V. Ivanova, E.O. Minyaylo, M.N. Temnikov, L.G. Mukhtorov, Y.M. Atroshchenko, Silicones in Cosmetics, Polym. Sci., Ser. B 65 (2023) 578–594, https://doi.org/10.1134/s1560090423600201.
[15] V.T.L. Tran, P. Gélin, C. Ferronato, J.M. Chovelon, L. Fine, G. Postole, Adsorption of linear and cyclic siloxanes on activated carbons for biogas purification: Sorbents regenerability, Chem. Eng. J. 378 (2019), https://doi.org/10.1016/j.cej.2019.122152.
[16] T. Mendiara, A. Cabello, M.T. Izquierdo, A. Abad, T. Mattisson, J. Adánez, Effect of the Presence of Siloxanes in Biogas Chemical Looping Combustion, Energy Fuel 35 (2021) 14984–14994, https://doi.org/10.1021/acs.energyfuels.1c02031.
[17] G. Flores-Salgado, J.A. Contreras, J. Pérez-Trevilla, G. Quijano, Removal of volatile methyl siloxanes in an anoxic two-phase partitioning bioreactor operated with hydrophobic biomass, Chem. Eng. J. 477 (2023) 146985, https://doi.org/10.1016/j.cej.2023.146985.
[18] L. Appels, J. Baeyens, R. Dewil, Siloxane removal from biosolids by peroxidation, EnergyConvers Manag 49 (2008) 2859–2864, https://doi.org/10.1016/j.enconman.2008.03.006.
[19] K. Oshita, K. Omori, M. Takaoka, T. Mizuno, Removal of siloxanes in sewage sludge by thermal treatment with gas stripping, Energy Convers Manag 81 (2014) 290–297, https://doi.org/10.1016/j.enconman.2014.02.050.
[20] J. Przepiórski, Chapter 9 Activated carbon filters and their industrial applications, in: Activated Carbon Surfaces in Environmental Remediation, 2006: pp. 421–474. doi: 10.1016/S1573-4285(06)80018-9.
[21] L. Rivera-Montenegro, E.I. Valenzuela, A. González-Sánchez, R. Muñoz, G. Quijano, Volatile Methyl Siloxanes as Key Biogas Pollutants: Occurrence, Impacts and Treatment Technologies, Bioenergy Res 16 (2023) 801–816, https://doi.org/10.1007/s12155-022-10525-y.
[22] A. Divsalar, L. Sun, M.N. Dods, H. Divsalar, R.W. Prosser, F.N. Egolfopoulos, T. T. Tsotsis, Feasibility of Siloxane Removal from Biogas Using an Ultraviolet Photodecomposition Technique, Ind. Eng. Chem. Res. 57 (2018) 7383–7394, https://doi.org/10.1021/acs.iecr.8b00710.
[23] R.-D. Sun, A. Nakajima, T. Watanabe, K. Hashimoto, Decomposition of gas-phase octamethyltrisiloxane on TiO2 thin film photocatalysts—catalytic activity, deactivation, and regeneration, J. Photochem. Photobiol. A Chem. 154 (2003) 203–209, https://doi.org/10.1016/S1010-6030(02)00322-2.
[24] L. Lamaa, C. Ferronato, S. Prakash, L. Fine, F. Jaber, J.M. Chovelon, Photocatalytic oxidation of octamethylcyclotetrasiloxane (D4): Towards a better understanding of the impact of volatile methyl siloxanes on photocatalytic systems, Appl Catal B 156–157 (2014) 438–446, https://doi.org/10.1016/j.apcatb.2014.03.047.
[25] A. Cabrera-Codony, M.A. Montes-Morán, M. Sánchez-Polo, M.J. Martín, R. Gonzalez-Olmos, Biogas upgrading: Optimal activated carbon properties for siloxane removal, Environ. Sci. Tech. 48 (2014) 7187–7195, https://doi.org/10.1021/es501274a.
[26] T. Matsui, S. Imamura, Removal of siloxane from digestion gas of sewage sludge, Bioresour. Technol. 101 (2010) S29–S32, https://doi.org/10.1016/j.biortech.2009.05.037.
[27] T. Matsui, S. Imamura, Removal of siloxane from digestion gas of sewage sludge, in: Bioresour Technol, Elsevier Ltd, 2010. doi: 10.1016/j.biortech.2009.05.037.
[28] G. Gatidou, O.S. Arvaniti, A.S. Stasinakis, N.S. Thomaidis, H.R. Andersen, Using mechanisms of hydrolysis and sorption to reduce siloxanes occurrence in biogas of anaerobic sludge digesters, Bioresour. Technol. 221 (2016) 205–213, https://doi.org/10.1016/j.biortech.2016.09.018.
[29] S.O. Hay, T.N. Obee, C. Thibaud-Erkey, The deactivation of photocatalytic based air purifiers by ambient siloxanes, Appl Catal B 99 (2010) 435–441, https://doi.org/10.1016/j.apcatb.2010.06.018.
[30] Z. Pan, L. Lin, W. Luo, The synthesis of a secondary branched epoxy-modified silicone resin and its application at low temperature, J. Appl. Polym. Sci. 141 (2024), https://doi.org/10.1002/app.55020.
[31] L.M. Johnson, L. Gao, C.W. Shields, M. Smith, K. Efimenko, K. Cushing, J. Genzer, G.P. López, Elastomeric microparticles for acoustic mediated bioseparations, J Nanobiotechnology 11 (2013), https://doi.org/10.1186/1477-3155-11-22.
[32] B. Thong-On, B. Rutnakornpituk, U. Wichai, M. Rutnakornpituk, Magnetite nanoparticle coated with amphiphilic bilayer surfactant of polysiloxane and poly (poly(ethylene glycol) methacrylate), J. Nanopart. Res. 14 (2012), https://doi.org/10.1007/s11051-012-0953-y.
[33] A.A. Belhekar, S.V. Awate, R. Anand, Photocatalytic activity of titania modified mesoporous silica for pollution control, Catal. Commun. 3 (2002) 453–458, https://doi.org/10.1016/S1566-7367(02)00179-6.
[34] J. Raskó, T. Kecskés, J. Kiss, Adsorption and reaction of formaldehyde on TiO2-supported Rh catalysts studied by FTIR and mass spectrometry, J. Catal. 226 (2004) 183–191, https://doi.org/10.1016/j.jcat.2004.05.024.
[35] S. Kwon, T.C. Lin, E. Iglesia, Elementary steps and site requirements in formic acid dehydration reactions on anatase and rutile TiO2 surfaces, J. Catal. 383 (2020) 60–76, https://doi.org/10.1016/j.jcat.2019.12.043.
[36] Y. Chen, Y. Park, H.G. Kang, J. Jeong, H. Kim, Chemical characterization and formation of secondary organosiloxane aerosol (SOSiA) from OH oxidation of decamethylcyclopentasiloxane, Environ. Sci.: Atmos. 3 (2023) 662–671, https://doi.org/10.1039/d2ea00161f.
[37] H.G. Kang, Y. Chen, Y. Park, T. Berkemeier, H. Kim, Volatile oxidation products and secondary organosiloxane aerosol from D5 + OH at varying OH exposures, Atmos, Chem. Phys. 23 (2023) 14307–14323, https://doi.org/10.5194/acp-23-14307-2023.
[38] R. Ellerbrock, M. Stein, J. Schaller, Comparing amorphous silica, short-range-ordered silicates and silicic acid species by FTIR, Sci. Rep. 12 (2022), https://doi.org/10.1038/s41598-022-15882-4.
[39] P. Krishnan, M. Liu, P.A. Itty, Z. Liu, V. Rheinheimer, M.H. Zhang, P.J.M. Monteiro, L.E. Yu, Characterization of photocatalytic TiO2 powder under varied environments using near ambient pressure X-ray photoelectron spectroscopy, Sci. Rep. 7 (2017), https://doi.org/10.1038/srep43298.
[40] N. Chen, Q. Lin, P. Zheng, J. Rao, Q. Zeng, J. Sun, A sustainable bio-based adhesive derived from defatted soy flour and epichlorohydrin, Wood Sci. Technol. 53 (2019) 801–817, https://doi.org/10.1007/s00226-019-01102-2.
[41] P. Su, J. Zhang, Y. Zhou, Z. Wei, S. Zhao, B. Yang, X. Zhao, J. Chen, Efficient photocatalytic production of hydrogen peroxide by Z-scheme resorcinol-formaldehyde resin/g-C3N4 heterostructure under visible light, Chem. Eng. J. 454 (2023) 140504, https://doi.org/10.1016/j.cej.2022.140504.
[42] J. Ma, J.H. Kim, J. Na, J. Min, G.H. Lee, S. Jo, C.S. Kim, Enhanced Polymerization and Surface Hardness of Colloidal Siloxane Films via Electron Beam Irradiation, ACS Omega 6 (2021) 13384–13390, https://doi.org/10.1021/acsomega.1c01429.
[43] Y. Wang, B. Wen, A. Dahal, G.A. Kimmel, R. Rousseau, A. Selloni, N.G. Petrik, Z. Dohnálek, Binding of Formic Acid on Anatase TiO2(101), J. Phys. Chem. C 124 (2020) 20228–20239, https://doi.org/10.1021/acs.jpcc.0c06031.
[44] L.T. Zhuravlev, The surface chemistry of amorphous silica, Zhuravlev Model, Colloids Surf A Physicochem Eng Asp 173 (2000) 1–38, https://doi.org/10.1016/S0927-7757(00)00556-2.
[45] Y. Choi, T. Kim, H. Lee, J. Park, J. Park, D. Ryu, W. Jeon, Bottom-up plasma-enhanced atomic layer deposition of SiO2 by utilizing growth inhibition using NH3 plasma pre-treatment for seamless gap-fill process, Sci. Rep. 12 (2022), https://doi.org/10.1038/s41598-022-20201-y.
[46] P. Post, L. Wurlitzer, W. Maus-Friedrichs, A.P. Weber, Characterization and applications of nanoparticles modified in-flight with silica or silica-organic coatings, Nanomaterials 8 (2018), https://doi.org/10.3390/nano8070530.
[47] T.L. Barr, An XPS study of Si as it occurs in adsorbents, catalysts, and thin films, Applications of Surface Science 15 (1983) 1–35, https://doi.org/10.1016/0378-5963(83)90003-X.
[48] D. Brassard, D.K. Sarkar, M.A. El Khakani, L. Quellet, Tuning the electrical resistivity of pulsed laser deposited TiSiOx thin films from highly insulating to conductive behaviors, Appl. Phys. Lett. 84 (2004) 2304–2306, https://doi.org/10.1063/1.1688999.
[49] Y. Sato, R. Hayami, T. Gunji, Characterization of NMR, IR, and Raman spectra for siloxanes and silsesquioxanes: a mini review, J Solgel Sci Technol 104 (2022) 36–52, https://doi.org/10.1007/s10971-022-05920-y.
[50] X. Qu, J. Lin, W. Qiang, C. Chen, D. Sun, Self-doped defect-mediated TiO2 with disordered surface for high-efficiency photodegradation of various pollutants, Chemosphere 308 (2022) 136239, https://doi.org/10.1016/j.chemosphere.2022.136239.
[51] P. Rychtowski, B. Tryba, A. Skrzypska, P. Felczak, J. Sreńscek-Nazzal, R.J. Wróbel, H. Nishiguchi, M. Toyoda, Role of the Hydroxyl Groups Coordinated toTiO2 Surface on the Photocatalytic Decomposition of Ethylene at Different Ambient Conditions, Catalysts 12 (2022), https://doi.org/10.3390/catal12040386.
[52] M.W. Alton, V.L. Johnson, S. Sharma, E.C. Browne, Volatile Methyl Siloxane Atmospheric Oxidation Mechanism from a Theoretical Perspective—How is the Siloxanol Formed? J. Phys. Chem. A 127 (2023) 10233–10242, https://doi.org/10.1021/acs.jpca.3c06287.
[53] I. Halasz, A. Kierys, J. Goworek, H. Liu, R.E. Patterson, 29Si NMR and Raman Glimpses into the Molecular Structures of Acid and Base Set Silica Gels Obtained

from TEOS and Na-Silicate, J. Phys. Chem. C 115 (2011) 24788–24799, https://doi.org/10.1021/jp207534e.
[54] H. Li, L. Chen, P. Duan, W. Zhang, Highly Active and Selective Photocatalytic Oxidation of Organosilanes to Silanols, ACS Sustain. Chem. Eng. 10 (2022) 4642–4649, https://doi.org/10.1021/acssuschemeng.2c00038.
[55] M.I. Mendoza Diaz, A. Balocchi, K. Oyekan, K. Tan, W.G. Vandenberghe, A. Esteve, C. Rossi, Dominant role of OH and Ti3+ defects on the electronic structure of TiO2 thin films for water splitting, Dalton Trans. 51 (2022) 15300–15311, https://doi.org/10.1039/D2DT01871C.
[56] K.H. Rahman, A.K. Kar, Hydroxylation-induced defect states and formation of a bidentate acetate adstructure of TiO2 catalysts with acetic acid variation for catalytic application, Semicond. Sci. Technol. 37 (2022) 045008, https://doi.org/10.1088/1361-6641/ac48dc.
[57] X. Kang, G. Dong, T. Dong, Oxygen Vacancy Defect Engineering of Heterophase Junction TiO2: Interfacial/Surface Oxygen Vacancies Coadjust the Photocatalytic ROS Production, ACS Appl. Energy Mater. 6 (2023) 1025–1036, https://doi.org/10.1021/acsaem.2c03535.
[58] R.P. Cavalcante, D.M. De Oliveira, L.D.M. Da Silva, J. Giménez, S. Esplugas, S.C. De Oliveira, R.F. Dantas, C. Sans, A. Machulek, Evaluation of the main active species involved in the TiO2 photocatalytic degradation of ametryn herbicide and its by-products, J. Environ. Chem. Eng. 9 (2021), https://doi.org/10.1016/j.jece.2021.105109.
[59] W.H. Saputera, H.A. Tahini, M. Sabsabi, T.H. Tan, N.M. Bedford, E. Lovell, Y. Cui, J.N. Hart, D. Friedmann, S.C. Smith, R. Amal, J. Scott, Light-Induced Synergistic Multidefect Sites on TiO2/SiO2 Composites for Catalytic Dehydrogenation, ACS Catal. 9 (2019) 2674–2684, https://doi.org/10.1021/acscatal.8b04891.
[60] J.S. Jeon, B.H. Kim, C.I. Park, S.Y. Seo, C. Kwak, S.H. Kim, S.W. Han, In-situ X-ray absorption fine structure study of TiO2 nanoparticles under ultraviolet light, Jpn. J. Appl. Phys. 49 (2010), https://doi.org/10.1143/JJAP.49.031105.